

# Spontaneous crystallographic instabilities of Pb nanoparticles in a SiO matrix

Avraham Be'er,<sup>1</sup> Richard Kofman,<sup>2</sup> Fritz Philipp,<sup>3</sup> and Yossi Lereah<sup>1</sup>

<sup>1</sup>*Department of Physical Electronics, Faculty of Engineering, Tel-Aviv University, Tel-Aviv 69978, Israel*

<sup>2</sup>*Laboratoire de Physique de la Matière Condensée, Unité Associée au CNRS 6622, Université de Nice, Parc Valrose, 06108 Nice Cedex 2, France*

<sup>3</sup>*Max Planck Institut für Metallforschung, Heisenbergstrasse 3, D-70569 Stuttgart, Germany*

(Received 27 March 2007; revised manuscript received 11 June 2007; published 8 August 2007)

The phenomenon of spontaneous instabilities of Pb nanoparticles was studied quantitatively by time-resolved transmission electron microscopy. The phenomenon rates were studied by high-resolution electron microscopy and by dark field microscopy. The origin of the phenomenon as a radiation effect of the high voltage electron beam was excluded by finding the same rates at 200 and 1250 kV electron beams, below and above the threshold for the knock-on process, respectively. The dependence of phenomenon rate on the particles' size was found to be inversely proportional to the particle volume. The temperature was found to influence both the probability for a particle to be in the unstable state and the rate of instabilities. The results are compared with our recent results obtained for spontaneous instabilities of Bi nanoparticles.

DOI: [10.1103/PhysRevB.76.075410](https://doi.org/10.1103/PhysRevB.76.075410)

PACS number(s): 61.46.Df

## I. INTRODUCTION

In the past two decades, it has been shown that nanoparticles of different materials change their crystallographic structure spontaneously under the transmission electron microscope beam.<sup>1-9</sup> Experimental and theoretical studies have pointed to either a quasimelting phenomenon,<sup>1,2</sup> in which random fluctuations between different structures appear, without melting, or rather the nanoparticle is completely melted by the electron beam for a short period, followed by recrystallization of a new structure.<sup>3</sup> Most of the experimental work was done on Au and Pb nanoparticles, and the atomic rearrangements, which were often called rotations, were described as the result of twin related transitions, typically to fcc metals. Lereah *et al.*<sup>4,5</sup> have extensively investigated by time-resolved high-resolution electron microscopy (HREM) the crystallographic rearrangements of Pb nanoparticles. In particular, they characterized the phenomenon as a twin related transition, and studied the rotation rate at room temperature. However, less is known about the quantitative influence of the temperature, the particle size, and the high voltage of the electron beam on the phenomenon. Recently, we have quantitatively shown<sup>10</sup> that the crystallographic rearrangement of Bi nanoparticles is thermally activated and occur by plane-after-plane gliding. It was shown that while the rotation rate depends on the particle volume and on the temperature, it does not depend on the high-voltage electron beam. In light of the above, we show, in this paper, quantitative results of the influence of the temperature, the particle size, and the high voltage of the electron beam on the phenomenon in Pb nanoparticles.

## II. EXPERIMENTAL SETUP

The experimental procedure was reported elsewhere<sup>10,11</sup>; here, we repeat the main features. Lead particles embedded in amorphous SiO were prepared by successive thermal evaporation in ultrahigh vacuum of 5 nm SiO (silicon monoxide SiO<sub>x</sub>, with  $x \sim 1$ ), 8 nm (as an average thickness) Pb,

and 10 nm SiO. Pb particles in various radii in the range of 1–10 nm were formed between the two SiO layers. Embedding the particles in SiO ensures better thermal coupling, which defines good thermodynamical variables and prevents oxidation, migration, and evaporation.<sup>11</sup>

The specimens were examined by transmission electron microscopy at 200 kV (Philips F20) and at 1250 kV (JEM-ARM1250), below and above the threshold (around 660 kV for Pb) for the knock-on process, respectively.<sup>12</sup> In both microscopes, the electron beam was expanded (in order to reduce sample heating) to create a fair signal in the camera. The order of magnitude of the flux was the same for both microscopes ( $\sim 1$  A/cm<sup>2</sup>), and the possible influence of the beam current on the phenomenon was discussed in Ref. 4. In both microscopes, the samples were examined at various temperatures, from liquid nitrogen temperature up to 175 °C. Records were obtained by HREM and by dark field (DF) microscopy. While quantifying the dependence of the phenomenon on the temperature, a deviation of the actual temperature, at the region under observation, from the measured one, is considered. Two origins exist for the deviation: the electron beam used for observation that heats locally the region under study and the poor heat conductivity of the thin film. The procedure for correcting the temperature measurements was described elsewhere.<sup>10</sup> The structure evolution of the particles was video recorded by an electron sensitive video camera with a time resolution of 25 frames/s, and the records were analyzed frame by frame.

## III. RESULTS

Pb particles in various radii in the range of 1–8 nm were analyzed at the above-mentioned two operated voltages, for the temperature range of –115 °C to 175 °C, by DF microscopy. The DF microscopy is obtained at a low magnification; therefore statistical analysis is reliable as many particles are included in the field of view. In the DF method, an aperture was positioned on the diffraction ring corresponding to (111) reflections. Rotations of the particles around the beam axis

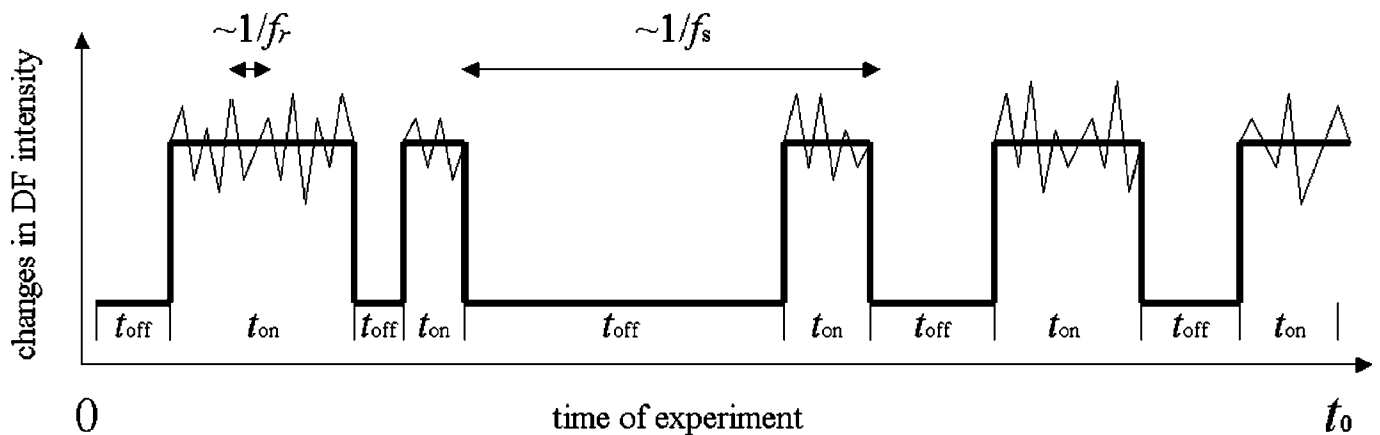


FIG. 1. The two intermittent states of a single nanoparticle under the e-beam, as was characterized due to changes of the DF intensity. The thick square line represents the two possible states: (a) stable state (“off” state), which lasts a typical time scale of  $t_{\text{off}}$ , and (b) rotating state (“on” state), which lasts a typical time scale of  $t_{\text{on}}$ . During the experiment time  $t_0$ , the particle switches between the states several times. During the rotating state (on state), the particle rotates between various crystallographic structures with a much higher rate than the switching rate, as presented by the thin broken line on top of the thick square line. The figure is schematic and does not represent real measured data.

are visible when the diffracted beam crosses the DF aperture’s borders, or alternatively, if the particles rotate around an axis perpendicular to the beam axis and go in and out of the Bragg condition. In the appropriate magnification, about 50 particles appear in a field of view.

The measurements show that each particle could be in one of the two following states: (a) stable state (“off” state), in which the particle reveals a constant white contrast, and (b) rotating state (“on” state), in which rotations are observed due to the intermittent (order of fraction of seconds) white and black contrast changes. The particles stay in each state a characteristic time of  $t_{\text{off}}$  and  $t_{\text{on}}$ , respectively, and then switch to the alternate state. The particles fluctuate between the two states several times during the experiment time  $t_0$  (order of few minutes), which is much larger than  $t_{\text{off}}$  and  $t_{\text{on}}$  (both of the order of few seconds), see Fig. 1. For each of the examined particles, an average of  $t_{\text{off}}$  and an average of  $t_{\text{on}}$ , during the experiment time  $t_0$ , were found in order to find a characteristic frequency of switching  $f_s = 1/(\langle t_{\text{off}} \rangle + \langle t_{\text{on}} \rangle)$  between the two states. The dependence of the probability  $P = \langle t_{\text{on}} \rangle / (\langle t_{\text{off}} \rangle + \langle t_{\text{on}} \rangle)$  of a particle to be in the rotating state on particle size, temperature, and electron energy was measured. The probability was measured by two methods: measuring along time for each individual particle and measuring the fraction of rotating particles at any moment. Measurements by the two methods resulted in a small deviation of 2%, indicating reliable statistics.

For each examined temperature, and for both electron energies,  $P$  drops to 0 at very large particle sizes, as these particles are in the solid state, and jumps to 1 at very small particles, which are already melted and do not fluctuate (or fluctuate at a faster rate than the camera detects). In between these borders, the probability of each particle to be in the rotating state decreases with size, as can be seen in Fig. 2. As the temperature rises, both borders are shifted to the right. At the left border, larger particles are now melted, while at the right border, particles that were at the solid state are now fluctuating. Similar results as in Fig. 2 were obtained also for 1250 kV.

For the particles located between the borders, the average probability  $\bar{P}$  was found to satisfy the relation  $\bar{P} = \bar{P}_0 \exp(-\Delta E_p/kT)$ , implying a thermal activation process with an activation energy of  $\Delta E_p = 0.02 \pm 0.003$  eV [Fig. 3(a)]. It is interesting to note that the probability increases with the temperature because of two reasons:  $t_{\text{on}}$  becomes longer, and  $t_{\text{off}}$  becomes shorter. The activation energy is needed to generate the process, and thus, it should be intuitively related to the changes of  $t_{\text{off}}$  with the temperature. Figure 3(b) represents the dependence of  $t_{\text{off}}$  on the temperature, showing an exponential dependence with the same activation energy as was found for  $\bar{P}$ . The characteristic frequency of switching  $f_s$  and  $t_{\text{on}}$  were found to be thermally activated as well, as can be seen in Fig. 3(b). The results presented in Fig. 3 show that changing the electron beams below and above the threshold for the knock-on process does not have any influence (within the experimental error) on the characteristic time scales,  $t_{\text{on}}$  and  $t_{\text{off}}$ , of the phenomenon, on the switching rate  $f_s$ , and on the probability  $\bar{P}$  to be in the rotating state.

At the rotating state, the dynamics of particles of different sizes (3.7–8 nm in radius) was analyzed for both electron energies at different temperatures using HREM. Using HREM, most of the particles’ configurations (90%) are characterized by the existence of twins. These twin structures are mainly single twin, microtwin, and multiple (3–5) twins. The particles fluctuate with time between configurations, while the crystalline structure (111) is visible at least in a part of the particle. The rotation is defined as a transition of the particle from a specific configuration to a new one (for more details on HREM measurements, and appropriate images, kindly see Refs. 5 and 10). The rotation rate was found to depend on the particle size: the smaller the particle is, the higher the rotation rate. The dependence of the rotation frequency  $f_r$  on particles size was plotted as a function of various powers of the particle radius  $R$ , revealing the best fitting factor (based on the square of the sample-correlation function of the linear fit) for the power of 3 (inset of Fig. 4). Figure 4 shows the rotation frequency obtained by HREM as

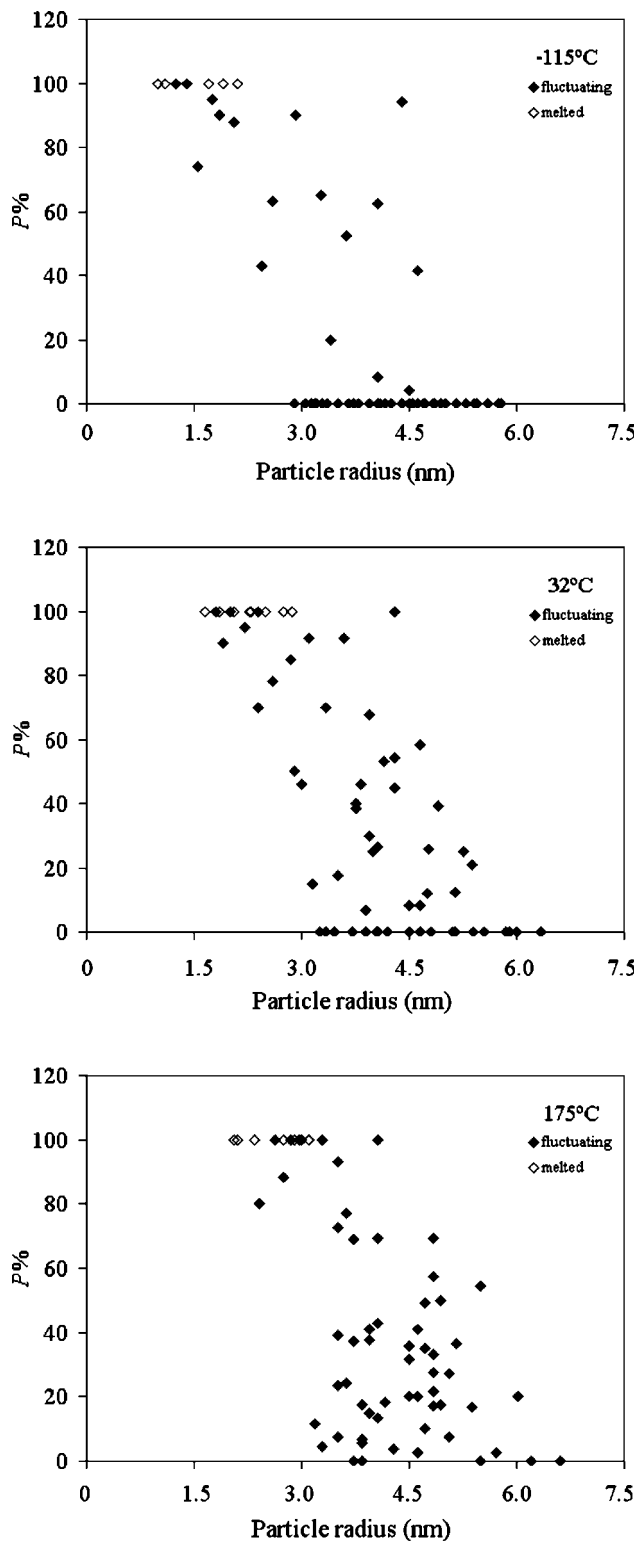


FIG. 2. The probability of a particle to be in the rotating state at 200 keV, for various particle radii at three chosen temperatures. Each dot represents a single particle. While at  $-115^\circ\text{C}$  the left and right borders are at 1.25 and 4.6 nm, respectively, at  $175^\circ\text{C}$  both borders have been significantly shifted to the right and are now at 2.4 and 6.0 nm, respectively. Notice how the number of  $P=0$  particles decreases while the temperature rises. The hollow dots represent the already totally melted particles obtained in the fields of view.

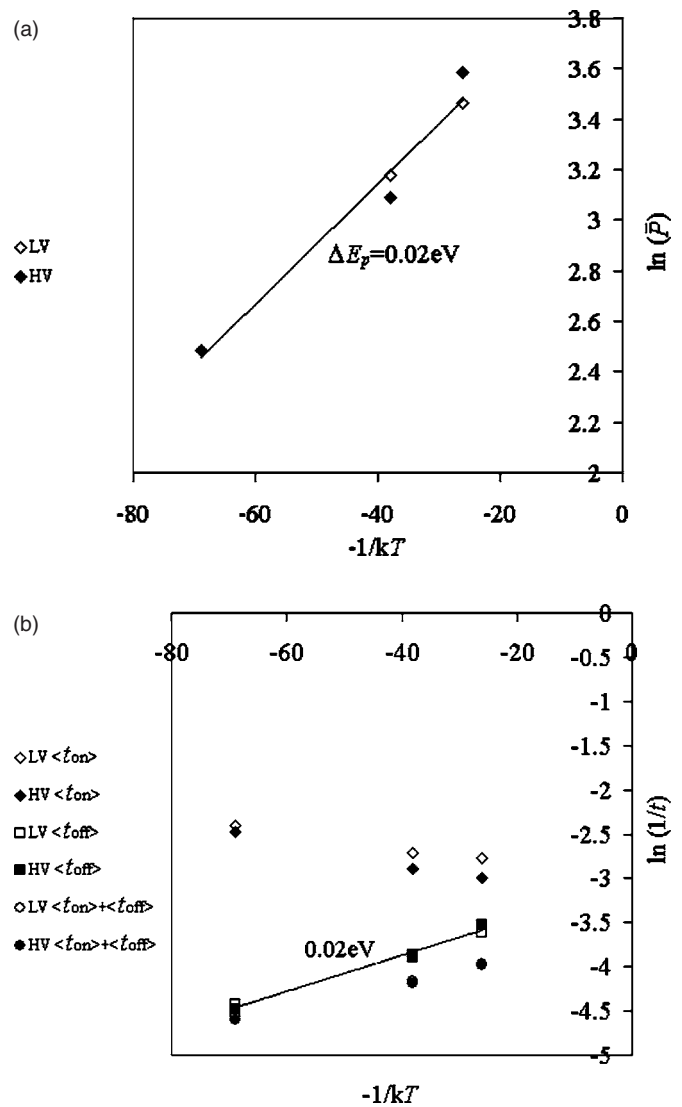


FIG. 3. (a) Linear behavior of  $\ln(\bar{P})$  as a function of  $-1/kT$ , for particles of different radii located between the borders, at the two operated high voltages, implying that  $\bar{P} = \bar{P}_0 \exp(-\Delta E_p/kT)$ , with  $\Delta E_p = 0.02 \text{ eV}$ . Notice the similarity between the results of the two voltages. (b) Linear behavior of the logarithm of  $t_{\text{off}}$ ,  $t_{\text{on}}$ , and  $f_s$  as a function of  $-1/kT$ , for particles of different radii located between the borders, at the two operated high voltages, implying a thermal activation process. The slope of  $t_{\text{off}}$  vs  $-1/kT$  was found to be equal to  $\Delta E_p = 0.02 \text{ eV}$ . Notice the similarity between the results of the two voltages.

a function of  $1/R^3$  for various temperatures. A cutoff of the rotation rate at the particle radius of 8 nm independent of temperature is observed. The following relation reflects the characteristic length scale of the phenomenon:

$$f_r(R) = C(T) \begin{cases} 1/R^3 - 1/R_0^3, & R < R_0 \\ 0, & R \geq R_0, \end{cases} \quad (1)$$

where  $R_0 = 8 \text{ nm}$ .  $C(T)$  is a temperature dependent constant, which, together with  $f_0$ , presented in Fig. 4, is discussed below.

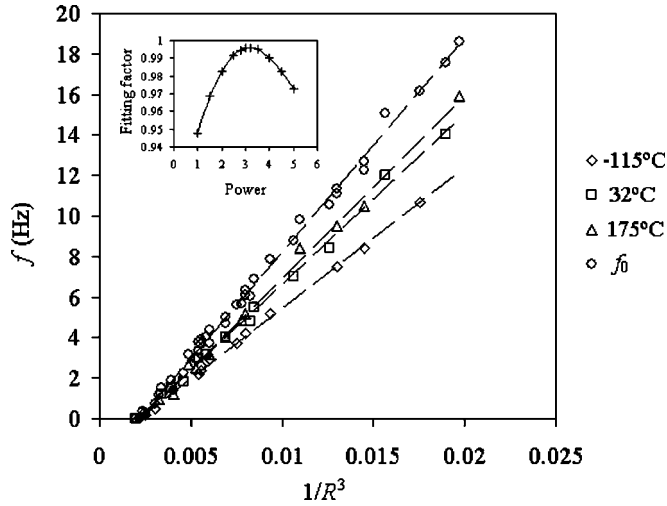


FIG. 4. Rotation frequency measured by HREM as a function of  $1/R^3$  for three temperatures:  $-115$ ,  $32$ , and  $175$  °C, at 200 keV, where  $f_0$  is the maximal frequency for a given particle with a radius  $R$ , calculated from Eq. (2). The cutoff at the particle radius of 8 nm is independent of the temperature, implying a characteristic length scale in the system. Inset: The accuracy of fitting a straight line to the graph of  $f_r$  vs  $1/R^\alpha$  for various values of  $\alpha$ .

Considering that the rotation rate  $f_r$  during the rotating state is also thermally activated:

$$f_r(T) = f_0 \exp(-\Delta E_f/kT), \quad (2)$$

the dependence of the rotation rate on the temperature indicates an activation energy  $\Delta E_f = 0.006 \pm 0.001$  eV, independent of the particle radius, where  $f_0$  is the maximal frequency for a given particle of radius  $R$ . The value of  $f_0$  was found from Eq. (2), as an average, by substituting various measured values of  $f_r$  and  $T$  for each  $R$ . It was found that also  $f_0$  is proportional to  $1/R^3 - 1/R_0^3$  (see Fig. 4); accordingly, we conclude that  $f_r(R, T) = A_0 f_r(R) f_r(T)$ , where  $C(T)$ , in Eq. (1) is  $\exp(-\Delta E_f/kT)$ , thus

$$f_r(R, T) = A_0 \exp(-\Delta E_f/kT) \begin{cases} 1/R^3 - 1/R_0^3, & R < R_0 \\ 0, & R \geq R_0, \end{cases} \quad (3)$$

where  $A_0$  is a constant.

The rotation rate  $f_r$  was found to be independent of the high voltage electron beam below and above the threshold for the knock-on process. Figure 5 shows the similarity between the rotation rate, measured by HREM, at room temperature for various particle sizes for both 200 and 1250 keV. The same similarity was obtained for other temperatures as well.

#### IV. DISCUSSION

Similar to our recent publication on the rearrangements of Bi nanoparticles,<sup>10</sup> we adapt the idea of Ajayan and Marks,<sup>1</sup> who proposed a scheme showing a deep energetic well followed by shallow ones. The particle, in their schematic description, is trapped in the deep well, and once out of the

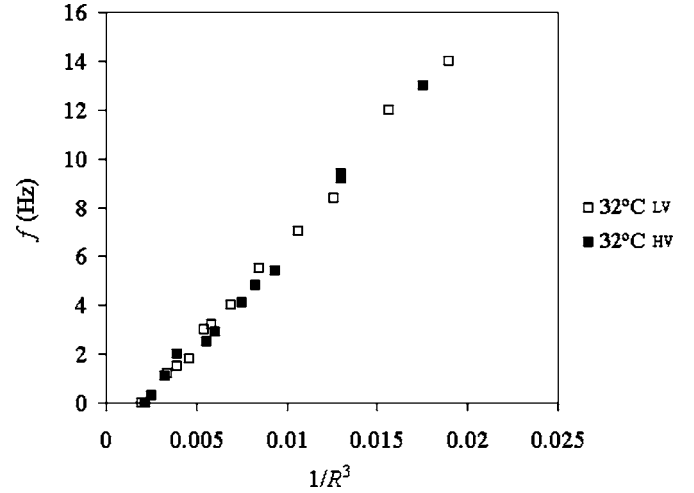


FIG. 5. Rotation frequency measured by HREM as a function of  $1/R^3$  at 32 °C for the two operation voltages: 200 and 1250 kV. The dots lay on the same line, indicating the irrelevance of the e-beam voltage.

well, can hop easily over the shallow morphological potential-energy surfaces. The energy gap  $\Delta E_p = 0.02$  eV between the stable and rotating states is the deep well, and  $\Delta E_f = 0.006$  eV is the shallow well, while the particle is in the rotating state. Quantitatively, we show that for Pb nanoparticles,  $\Delta E_p/\Delta E_f \approx 3.5$ . The calculated activation energies (0.02 and 0.006 eV), compared with 0.025 eV of room temperature, indicate that the driving force stems from the ambient temperature. However, the values obtained here for both the deep ( $\Delta E_p = 0.02$  eV) and shallow ( $\Delta E_f = 0.006$  eV) energetic wells are recognizably smaller than those obtained for Bi particles,<sup>10</sup> i.e.,  $\Delta E_p = 0.08$  eV and  $\Delta E_f = 0.017$  eV. This might point to the different bonding types, which is also manifested via a sort of a boundary defect, low energetic twin defects for Pb (fcc) particles, and higher energetic planar defects, as extensively explained in Ref. 10, for Bi (rhombohedral) particles. It is also interesting to note that the particles' threshold sizes ( $R_0 = 8$  nm for Pb and  $R_0 = 5$  nm for Bi), above which the particles are stable, are recognizably different as well, implying smaller surface stresses in the Pb particles, which yield the need of a lower amount of external energy for the instability process. The idea of Auger electrons,<sup>3</sup> on the other hand, where it is argued that the nanoparticles are melted, is not compatible with our results since our HREM show that no melting takes place.<sup>5,10</sup>

#### V. SUMMARY

In summary, we have quantified the time scales and the probability of a particle to be in the rotating state in the process of spontaneous instability of Pb nanoparticles, under the electron beam, for various temperatures and particle sizes. The origin of the phenomenon as a radiation effect of the high-energy electron beam was excluded. The rotation rate was found to be inversely proportional to the particle

volume, up to a threshold size, above which the particles are stable. The temperature was found to activate both the probability of a particle to be in the rotating state and the rotation rate. Our results suggest that inner bonding interactions inside Pb nanoparticles are recognizably smaller from those existing in Bi nanoparticles.

#### ACKNOWLEDGMENTS

We thank R. Höschel for assistance with high-voltage electron microscopy. This work was partially supported by the German Israeli Foundation (GIF). A.B. thanks the Israeli Ministry of Science for their support.

- 
- <sup>1</sup>P. M. Ajayan and L. D. Marks, *Phys. Rev. Lett.* **63**, 279 (1989).  
<sup>2</sup>P. M. Ajayan and L. D. Marks, *Phys. Rev. Lett.* **60**, 585 (1988).  
<sup>3</sup>P. Williams, *Appl. Phys. Lett.* **50**, 1760 (1987).  
<sup>4</sup>Y. Lereah, R. Kofman, J. M. Penisson, G. Deutscher, P. Cheyssac, T. Ben David, and A. Bourret, *Philos. Mag. B* **81**, 1801 (2001).  
<sup>5</sup>T. Ben-David, Y. Lereah, G. Deutscher, J. M. Penisson, A. Bourret, R. Kofman, and P. Cheyssac, *Phys. Rev. Lett.* **78**, 2585 (1997).  
<sup>6</sup>S. Iijima and T. Ichihashi, *Phys. Rev. Lett.* **56**, 616 (1986).  
<sup>7</sup>L. D. Marks, *Rep. Prog. Phys.* **57**, 603 (1994).  
<sup>8</sup>J.-O. Bovin, R. Wallenberg, and D. J. Smith, *Nature (London)* **317**, 47 (1985).  
<sup>9</sup>W. Krakow, M. Jose-Yacaman, and J. L. Aragon, *Phys. Rev. B* **49**, 10591 (1994).  
<sup>10</sup>A. Be'er, R. Kofman, F. Phillipp, and Y. Lereah, *Phys. Rev. B* **74**, 224111 (2006).  
<sup>11</sup>R. Kofman, P. Cheyssac, R. Garrigos, Y. Lereah, and G. Deutscher, *Z. Phys. D: At., Mol. Clusters* **20**, 267 (1991).  
<sup>12</sup>K. Urban, *Phys. Status Solidi A* **56**, 157 (1979).